ENHANCED METHODS
OF SEASONAL ADJUSTMENT

By D.S.G. Pollock

University of Leicester

Email: stephen_pollock@sigmapi.u-net.com

The effect of the conventional model-based methods of seasonal adjustment is to nullify the elements of the data that reside at the seasonal frequencies and to attenuate the elements at the adjacent frequencies. It may be desirable to nullify some of the adjacent elements instead of merely attenuating them. For this purpose, two alternative procedures are presented that have been implemented in a computer program.

In the first procedure, the seasonal-adjustment filter is augmented by additional filters that are targeted at the adjacent frequencies. In the second procedure, a Fourier transform is deployed to reveal the elements of the data at all the frequencies. This allows the elements in the vicinities of the seasonal frequencies to be eliminated or attenuated at will.

In spite of the success of these procedures, the question is raised of whether the estimated trend-cycle trajectory that is devoid of high-frequency noise can serve in place of the seasonally adjusted data.

Introduction

This paper discusses some existing and some newly proposed methods for the seasonal adjustment of economic data.

Two sets of methods are used preponderantly, at present, by central statistical offices. These are the heuristic methods that comprise the venerable X-11 procedure of Shiskin, Young and Musgrave (1967) and its derivatives and the newer model-based methods that are represented primarily by the SEATS TRAMO package of Augustin Maravall—see Gómez and Maravall (1997) and Caporello and Maravall (2004). A broad perspective on model-based business-cycle analysis and seasonal adjustment has been provided by Kaiser and Maravall (2001).

Both sets of methods, which operate in the time domain, are complicated and difficult to master, albeit that they are nowadays accompanied by helpful online guidance. The X-11 program is well served by the monograph of Ladiray and Quenneville (2001). However, problems can arise with these methods that can be overcome by methods that operate in the frequency domain.

The traditional procedures that are based on the X-11 program were informed by a limited theory of filtering, which can be improved on. The model-based methods are the products of a dominant opinion amongst economists that economic investigations should be conducted within the context of well-defined models of economic activities. A difficulty with this opinion is that the models are sometimes incapable of capturing the complexities of the economic data. They can lead to distorted views of economic reality and to other failures when the models cannot be

fitted adequately to the data. This can happen when the data are too heterogenous to sustain a model with fixed parameters.

Another problem that affects the time-domain methods of seasonal adjustment is that they nullify completely only the elements at the seasonal seasonal frequency and its harmonics. The seasonal fluctuations may comprise elements at adjacent frequencies that also need to be removed from the data.

A testimony to this problem has been provided by McElroy and Roy (2017), who have provided a means of detecting residual seasonal effects in seasonally adjusted date. The issue has also been raised by Findley *et al.* (2005). The present paper describes some means of addressing the problem that operate in the time domain and in the frequency domain.

The ultimate purpose has been to build a program that comprises both some amended versions of the time-domain procedures and a full set of frequency-domain procedures. Then, the two sets of procedures will bear mutual comparison.

Comb Filters

Any time-domain procedure for seasonal adjustment must contain a component that acts in the manner of a comb filter. This filter is a rational polynomial function of the lag operator, albeit that it can be represented as a ratio of two polynomials of which the argument is a complex number z. Thus, the comb filter will be represented by

$$\frac{\Sigma(z)}{P(z)} = \frac{1 + z + z^2 + \cdots + z^{s-1}}{1 + \rho z + (\rho z)^2 + \cdots + (\rho z)^{s-1}} = \frac{(1 - z^s)(1 - \rho z)}{(1 - z)(1 - \rho^s z^s)}, \qquad (1)$$

where $\rho \in (0, 1)$ and where $s = 4, 12$ denotes either a quarterly or a monthly frequency of observation. Here, the numerator polynomial contains zeros at the seasonal frequencies, which are $\omega_j = 2\pi j/s; j = 1, 2, \ldots, s - 1$. These are amongst the roots of the equation $1 - z^s = 0$, which are the so-called roots of unity (The zero at the angle $\omega_0 = \omega_s$ is excluded.)

The poles that accompany the zeros are provided by the solution to the equation $1 - \rho^s z^s = 0$, where $\rho < 1$ is close to unity. These are the roots of the denominator polynomial of the filter. The poles take the values $\rho \exp(\mathrm{i}2\pi j/s)$; $j = 1, 2, \ldots, s - 1$, which is to say that they lie on a circle in the complex plane of radius ρ^{-1}. Figure 1 depicts the poles and the zeros of the comb filter, albeit that, for graphical purposes, the argument z of the polynomials has been replaced by z^{-1}, to keep the poles within the unit circle.

The nullification of the seasonal elements of the data is achieved by the zeros of the filter. The effects of these zeros at other frequencies is limited by the presence of the poles of the filter that lie on the same axes or radii as the zeros and that are close to the unit circle. At frequencies that are remote from the seasonal frequencies, the effects of the poles and the zeros are largely cancelled.
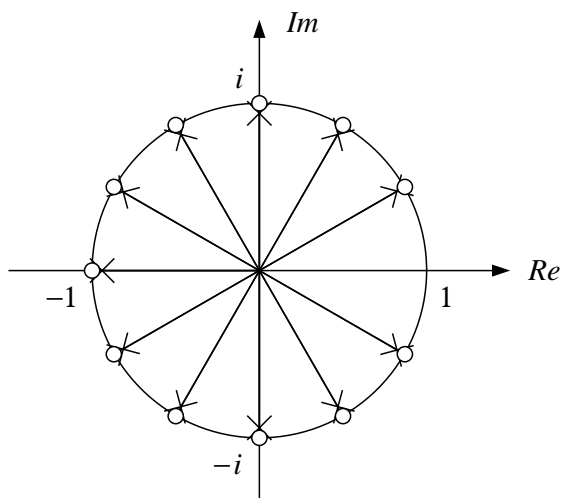
Figure 1. The pole-zero diagram of the unidirectional comb filter for monthly data. The poles are marked by crosses and the zeros are marked by circles.

The filter of equation (1) is unidirectional and backward looking, such that the filtered values will be formed from past and present values of the data. The filter will, therefore, induce a phase shift or a time lag in the processed data.

To avoid such an effect, the filter must reach equally forwards and backwards in time. For this reason, it is appropriate adopt a bidirectional filter of the form

$$B(z) = \mu \frac{\Sigma(z^{-1})\Sigma(z)}{P(z^{-1})P(z)}. \tag{2}$$

Here, μ if a factor that is adjusted to ensure that the value of $B(z)$ is unity when at $z = 1$. This will ensure that the filter preserves the level of the data.

The effect of the filter is revealed by its frequency response function, which shows the manner in which the filter modifies the amplitudes of the sinusoidal elements of which the data is composed. It is obtained by setting $z = \exp\{-i\omega\}$ and by running ω from zero to the limiting frequency of π. The frequency response of the monthly comb filters with $\rho = 0.8$ and $\rho = 0.9$ is shown in Figure 2.

The expansion of the rational function of (2) will give rise to a doubly-infinite sequence of coefficients. Therefore, the filter cannot be applied directly to a finite sequence of data, unless one is prepared to truncate the sequence of coefficients. Instead, the filter may be applied in two passes running through the data in opposite directions.

These processes can be represented by the equations

$$P(z)q(z) = \Sigma(z)y(z) \qquad \text{and} \qquad P(z^{-1})x(z) = \Sigma(z^{-1})q(z), \tag{3}$$
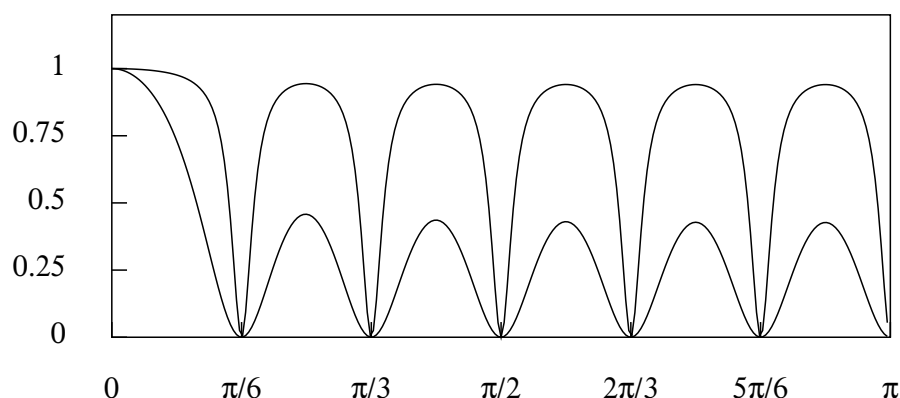
Figure 2. The frequency response function of the bidirectional comb filter for monthly data with $\rho = 0.8$, giving the lesser peaks, and $\rho = 0.9$, giving the higher peaks.

where $y(z) = \sum y_t z^t$ is the z-transform of the data sequence $y(t) = \{y_t; t = 0 \pm 1, \pm 2, \ldots\}$, where $q(t)$ is an intermediate sequence generated by the forward pass of the one-sided filter of (1) and where $x(t)$ is the final filtered sequence resulting from the backwards pass of the filter. In order to initiate the forwards and backwards passes, it is necessary to supply some initial conditions, to be obtained by backcasting and forecasting the elements of $y(t)$ and $q(t)$ respectively.

Wiener–Kolmogorov Filters

A problem with the filter of (2) is the manner in which the peaks of the frequency reponse function that lie between the seasonal frequencies are diminished. Ideally, they should reach values close to unity so that the non-seasonal elements of the data can be largely preserved. Also, this filter offers little control over the width of the clefts that surround the seasonal frequencies.
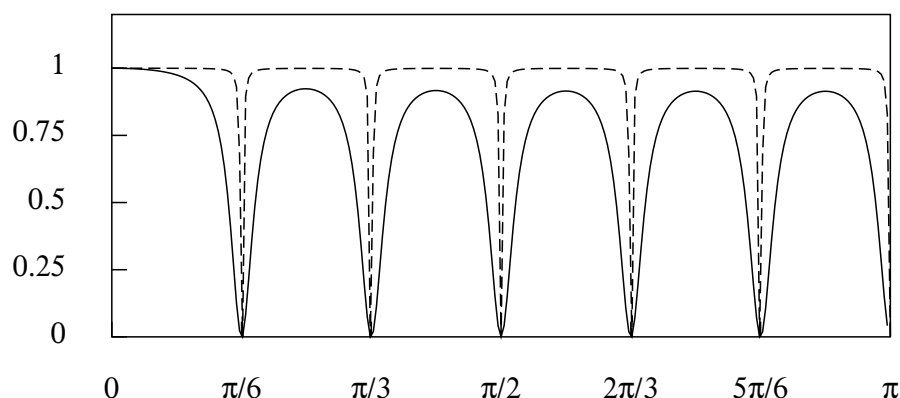

Figure 3. The frequency response functions of the ordinary seasonal adjustment filter for monthly data with $\lambda = 0.5.$ and $\rho = 0.8$ (the solid line) and with $\lambda = 0.5.$ and $\rho = 0.99$ (the dashed line).

These problems can be overcome by adopting a Wiener–Kolmogorov formula-

tion that gives rise to the following filter:

$$\Psi(z) = \mu \frac{\Sigma(z^{-1})\Sigma(z)}{\Sigma(z^{-1})\Sigma(z) + \lambda P(z^{-1})P(z)}. \tag{4}$$

Figure 3 shows the frequency response function of two such filters, wherein the parameter values are $\rho = 0.99$ and $\lambda = 0.5$, which give rise to a frequency response function with narrow clefts at the seasonal frequencies, and $\rho = 0.8$ and $\lambda = 0.5$, which give rise to one with wide clefts.

The Wiener–Kolmogorov filters are commonly derived from statistical models comprising additive components. In this context, the filtered data represent a minimum-mean-square-error estimate of one or other the components of the model.

An heuristic model that gives rise to the filter of (4) is represented in a z-transform notation by

$$\begin{aligned} y(z) &= \frac{P(z)}{\Sigma(z)}\nu(z) + \eta(z) \\ &= \xi(z) + \eta(z), \end{aligned} \tag{5}$$

where $y(z) = \sum y_t z^t$ is the z-transform of the stochastic sequence $y(t) = \{y_t; t = 0 \pm 1, \pm 2, \ldots\}$, and where $\xi(z)$, $\eta(z)$ and $\nu(z)$ are defined likewise.

Here, $\xi(z)$ represents the seasonal fluctuations, whereas $\eta(z)$ represents whatever other motions may be present in the detrended data. Both $\nu(z)$ and $\eta(z)$ stand for mutually independent white-noise processes with variances of σ_ν^2 and σ_η^2, respectively.

It would be possible to elaborate the representation of the non-seasonal process $\eta(t)$ by making it the product of an autoregressive moving-average process. However, the purpose of the model is not to provide a realistic representation of the process to be filtered. Instead, the model is to be regarded solely as a means of deriving an appropriate filter.

It is notable that the model has no trend function. Whatever trend there may be in the data to filtered can be removed, usually, by interpolating a polynomial function of an appropriate degree into the data. In that case, $y(z)$ will correspond to the residuals of a polynomial regression.

The presence of complex roots of unit modulus within the polynomial $\Sigma(z)$ implies that the process $y(t)$ is non-stationary in amplitude. It may be reduced to stationarity by multiplying throughout by $\Sigma(z)$ to give

$$\begin{aligned} \Sigma(z)y(z) &= P(z)\nu(z) + \Sigma(z)\eta(z) \\ &= \delta(z) + \kappa(z) = g(z). \end{aligned} \tag{6}$$

The conditional expectation $\eta(z)$ given $g(z)$ is

$$E\{\eta(z)|g(z)\} = E\{\eta(z)\} + \frac{C\{\eta(z), g(z)\}}{V\{g(z)\}}[g(z) - E\{g(z)\}]. \tag{7}$$

5

Give that

$$V\{g(z)\} = \sigma_\nu^2 P(z^{-1})P(z) + \sigma_\eta^2 \Sigma(z^{-1})\Sigma(z) \qquad \text{and}$$

$$C\{g(z), \eta(z)\} = \sigma_\eta^2 \Sigma(z),$$

(8)

and given that $E\{\eta(z)\} = E\{g(z)\} = 0$, it follows that

$$E\{\eta(z)|g(z)\} = \frac{\Sigma(z^{-1})\Sigma(z)}{\Sigma(z^{-1})\Sigma(z) + \lambda P(z^{-1})P(z)} y(z) = \Psi(z)y(z),$$

(9)

where $\lambda = \sigma_\nu^2/\sigma_\eta^2$. It will be recognised that $\Psi(z)$ is the ratio of the autocovariance generating function of the component to be estimated to that of the data sequence.

In order to apply the filter in a bidirectional manner, it is necessary to factorise the denominator as the product of a factor in z, to be used in the forwards pass, and a factor in z^{-1}, to be used in the backwards pass. There is also a need to supply initial conditions for both processes. These difficulties can be overcome by adopting a genuine finite-sample version of the filter.

The Finite-Sample Wiener–Kolmogorov Filter

To derive the finite-sample version of the Wiener–Kolmogorov filter, consider a vector $y = [y_0, y_1, \ldots, y_{T-1}]'$ of T values drawn from the process represented by $y(z)$. In accordance with equation (5), the vector may be decomposed as

$$y = \xi + \eta.$$

(10)

The finite-sample version of the filter of (9) will be a matrix transformation of order T that maps from the data vector y to a vector h that represents the estimate of η. To derive such a transformation, one can begin by finding the matrix analogues of the operators $\Sigma(z)$ and $P(z)$.

These matrices can be obtained by replacing the argument z by the matrix lag operator $L_T = [e_1, \ldots, e_{T-1}, 0]$ of order T, which is derived from the identity matrix $I_T = [e_0, e_1, \ldots, e_{T-1}]'$ by deleting the leading column and by adding a column of zeros to the end of the array.

The resulting matrices, denoted by $\Sigma_T = \Sigma(L_T)$ and $P_T = P(L_T)$ are lower-triangular. The matrices corresponding to $\Sigma(z^{-1})$ and $P(z^{-1})$ are the upper triangular matrices Σ_T' and P_T' respectively.

With the matrix operators in place of the polynomial operators, the following matrix transformation is derived:

$$h = \Sigma_T'(\Sigma_T\Sigma_T' + \lambda P_T P_T')^{-1}\Sigma_T y.$$

(11)

It is notable that the first $s-1$ elements of $\Sigma_T y$ differ from the remaining elements in so far as they comprise fewer than s elements of the data vector. To supply the missing elements, some pre-ample values of the data might be generated.

An alternative recourse is to discard the first $s-1$ elements of the transformation. Consider the following equations

$$\Sigma(L_T)y = \begin{bmatrix} S_*' \\ S' \end{bmatrix} y = \begin{bmatrix} g_* \\ g \end{bmatrix}, \qquad P(L_T)x = \begin{bmatrix} R_*' \\ R' \end{bmatrix} x = \begin{bmatrix} z_* \\ z \end{bmatrix}.$$

(12)

The effect of discarding the subvectors g_* and z_* can be achieved by replacing Σ_T and P_T by S' and R' respectively. Then, the matrix analogue of the filter equation becomes

$$h = \Psi y = S(S'S + \lambda R'R)^{-1}S'y. \tag{13}$$

This equation can also be derived from a conditional expectation. Applying S' to the equation $y = \xi + \eta$, representing the seasonally fluctuating data, gives

$$S'y = R'\nu + S'\eta$$
$$= \delta + \kappa = g. \tag{14}$$

This is just a segment of $T - s$ elements drawn from the process represented by equation (6).

The expectations and the dispersion matrices of the component vectors of g are

$$E(\delta) = 0, \qquad D(\delta) = \sigma_\nu^2 R'R,$$
$$E(\kappa) = 0, \qquad D(\kappa) = \sigma_\eta^2 S'S. \tag{15}$$

The conditional expectation of η, given the transformed data $g = S'y$, is provided by the formula

$$h = E(\eta|g) = E(\eta) + C(\eta, g)D^{-1}(g)\{g - E(g)\}$$
$$= C(\eta, g)D^{-1}(g)g, \tag{16}$$

where the second equality follows in view of the zero-valued expectations of η and g. Within this expression, there are

$$D(g) = \sigma_\nu^2 R'R + \sigma_\eta^2 S'S \quad \text{and} \quad C(\eta, g) = \sigma_\eta^2 S. \tag{17}$$

Putting these details into (16) gives the following estimate of η:

$$h = \sigma_\eta^2 S(\sigma_\nu^2 R'R + \sigma_\eta^2 S'S)^{-1}S'y$$
$$= S(S'S + \lambda R'R)^{-1}S'y, \tag{18}$$

where $\lambda = \sigma_\nu^2/\sigma_\eta^2$.

A simple procedure for calculating h begins by solving the equation

$$(S'S + \lambda R'R)b = S'y = g \tag{19}$$

for the value of b. Thereafter, one can generate $h = Sb$.

The solution to equation (19) may be found via a Cholesky factorisation that sets $S'S + \lambda R'R = LDL'$, where L is a lower-triangular matrix with a limited number of nonzero bands and D is a diagonal matrix. The system $LDL'b = g$ may be cast in the form of $Lp = g$ and solved for p. Then, $L'b = D^{-1}p$ can be solved for b, whence $h = Sb$ can be derived.

It will be observed that the equation (18) can also be written as

$$h = (SL'^{-1})D^{-1}(L^{-1}S')y, \tag{20}$$

where SL'^{-1} is an upper-triangular matrix, and where its transpose $L^{-1}S'$ is a lower-triangular matrix. This equation corresponds to a method of bi-directional filtering in which $p = L^{-1}S'y$ represents a real-time filtering and $h = SL'^{-1}D^{-1}p$ represent a reverse-time filtering, which is also described as a smoothing operation.

The transformation $h = \Psi y$ of (13) and (18) entails a bi-symmetric matrix (which is symmetric with respect to both the NW–SE and the NE–SW diagonals).

One consequence of this characteristic is that the outcome is invariant with respect to the reversal of the order of the element in the vectors y and h. Thus, if the reversed vectors are denoted by $y^\# = Jy$ and $h^\# = Jh$, where J is a matrix with units on the NE–SW diagonal and with zeros elsewhere, then $h^\# = \Psi y^\#$. That is not the case for the transformation of (11).
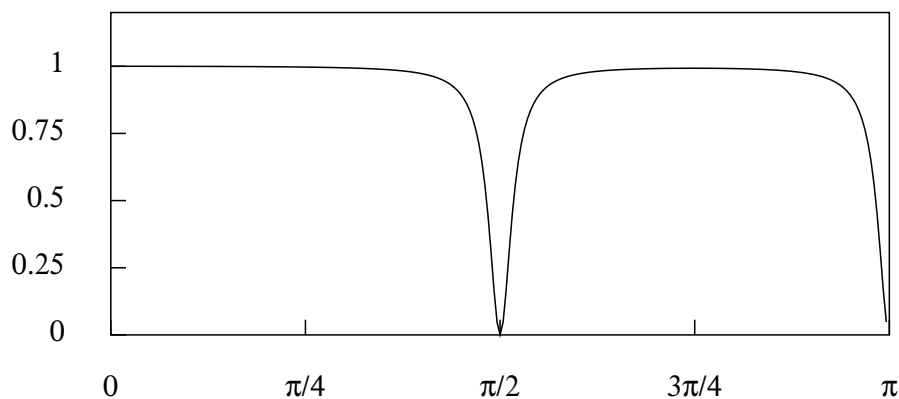

Figure 4. The frequency response functions of the ordinary seasonal adjustment filter for quarterly data with $\lambda = 0.5$. and $\rho = 0.9$).
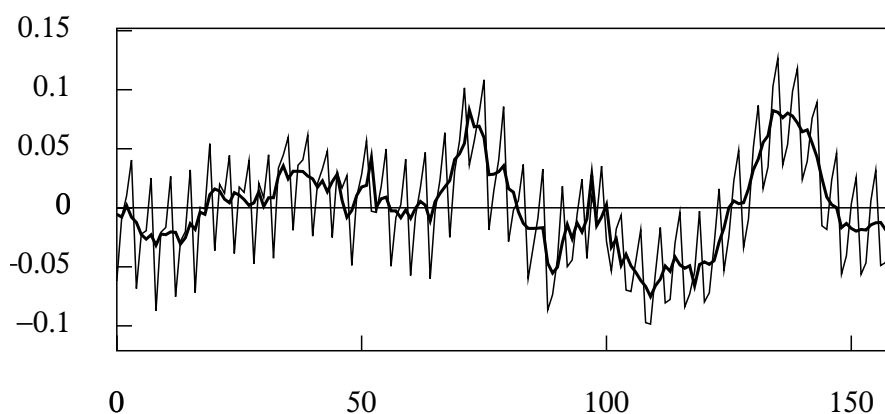

Figure 5. The residuals from a linear detrending of the logarithms of an index of quarterly U.K. Consumption for the years 1955 to 1994, with a superimposed seasonally adjusted sequence.

Figure 4 shows the frequency response function of the seasonal adjustment filter for quarterly data and Figure 5 shows the effect of applying the quarterly seasonal filter to the residuals from a linear detrending of the logarithms of an index of quarterly U.K. Consumption for the years 1955 to 1994. Figure 6 shows the seasonal component that has been extracted from these data.

The seasonally adjusted data of Figure 5 have a rough and irregular profile that contrasts markedly with the regularity of the seasonal component. That regularity is unsurprising in view of the fact that the component comprises a restricted set of seasonal elements consisting only of those at the fundamental seasonal frequency and at its harmonic frequency, together with some severely attenuated elements at the adjacent frequencies.
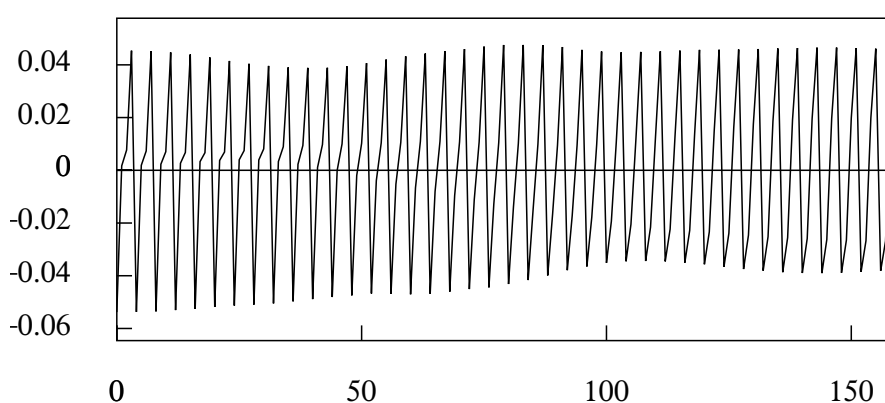

Figure 6. The seasonal component extracted from the logarithms of an index of quarterly U.K. Consumption for the years 1955 to 1994.

One might wish for a smoother version for the trajectory of the seasonally adjusted data. Such trajectories are shown in figures 12 and 14, where they are designated as trend-cycle functions. They are accompanied by seasonally fluctuating residual sequences that are much rougher than that of Figure 6.

Lying within the data, between the regular series of seasonal fluctuations and the smooth trend-cycle function, will be a rough and irregular sequence that is liable to be regarded as noise that is fit to be discarded, unless it shows some correlation with other economic variables.

A smooth trend-cycle function can be created by applying the time-domain Butterworth filter to the data. The residual deviations of the data from the trend-cycle trajectory can be subjected to a seasonal adjustment procedure to create a seasonal component and a residual component, which is the putative noise.

Widening the Seasonal Stopbands

Figure 3 shows the ordinary seasonal adjustment filter for monthly data when the smoothing parameters is $\lambda = 0.5$ and the pole parameter is $\rho = 0.8$. There is a complete nullification of the elements at the seasonal frequencies; and those at the adjacent frequencies are attenuated to an extent that diminishes rapidly as their distance from the seasonal frequencies increases.

To increase the attenuation of the elements of the data that are adjacent to the seasonal frequencies, one can reduce the value of ρ within the polynomial $P(z)$. This will draw the poles away from the unit circle, with an effect that can be seen by comparing the two functions that are plotted in of Figure 3.

It may be required to impose a greater attenuation on the adjacent elements than can be achieved by reductions in the value of ρ, and it may be desirable to confine this effect more narrowly to the vicinities of the seasonal frequencies.

For this purpose, it might be appropriate to apply the seasonal-adjustment filter twice or more in succession and with poles and zeros that are displaced from the seasonal frequencies by small angles. A twofold filter with equal displacements on either side of the seasonal frequencies could take the form of

$$\Psi_\zeta(\omega) = \Psi(\omega - \zeta)\Psi(\omega + \zeta), \tag{21}$$

where ζ is the angle of the displacement. It should be observed that $\cos(\pi + \zeta) = \cos(\pi - \zeta)$. Thus, the same factor is present in both $\Psi(\omega - \zeta)$ and $\Psi(\omega + \zeta)$. To avoid the duplication, it is reasonable to exclude the factor from the first of these filters.
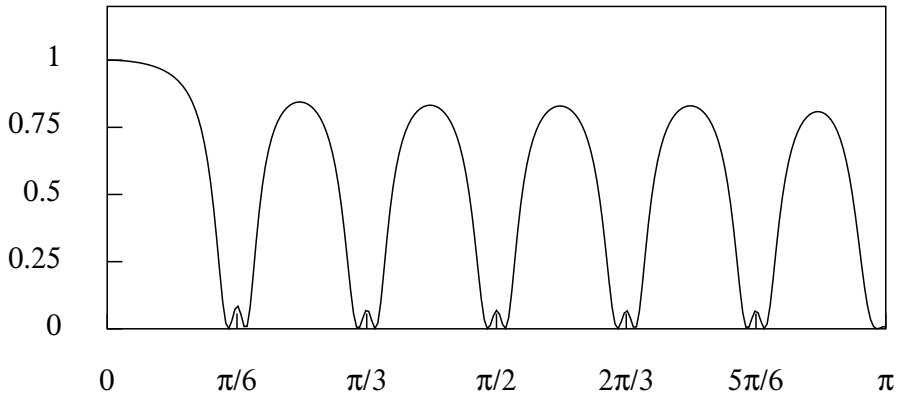

Figure 7. The frequency response function of the double seasonal adjustment filter for monthly data with offsets of 2 degrees.

75 shows the frequency response of the resulting double filter in which the offsets are $\pm\zeta = \pm 2$ degrees (0.0349 radians). The lack of zeros at the seasonal frequencies allows a small amount of leakage to occur, which increases with the size of the offsets and with the value of ρ. Given the likely prominence of the elements of the data at the seasonal frequencies, this leakage is liable to prove problematic.

To overcome the leakage of the double filter, it is possible to combine the standard filter with the two offset filters to create a triple filter. The first and primary filter will have its poles and zeros at exactly the seasonal frequencies. The second and the third of the filters will have their poles and zeros offset to the left and to the right, respectively. Moreover, it may be desirable to apply differing offsets relative to some or all of the seasonal frequencies.

Thus, if it were required to place additional poles and zeros on either side of the frequencies ω_j, then it would be appropriate to compound the denominator

polynomials $P(z)$ of the offset filters from the factors

$$1 - 2\rho\cos(\omega_j + \zeta_1)z + \rho^2 z^2 \quad \text{and} \quad 1 - 2\rho\cos(\omega_j - \zeta_2)z + \rho^2 z^2 \qquad (22)$$

and to compound their numerator polynomials $\Sigma(z)$ from similar factors, but with $\rho = 1$.

The appropriate displacements can be determined with reference to the periodogram of the seasonal data after their trend has been removed. This will indicate which of the data elements adjacent to the seasonal elements should be taken into account, to be eliminated or attenuated.

The frequency response of such a triple filter is illustrated in Figure 8. Here, the values of $\lambda = 0.5$ and $\rho = 0.8$, which have characterised the previous filters, are retained. However, an offset of 3 degrees (0.0524 radians) has been applied on either side of each of the seasonal frequencies.

A problem with the frequency response of the triple filter is that its values at the midpoints between the seasonal frequencies are significantly less that unity. This conflicts with the intention of preserving the elements of the data at these points and in the vicinities thereof. There is also an uncomfortable degree of leakage in the wide stop bands of the filter. Similar but a less severe problems also arises with the double filter. These problems can be overcome by operating in the frequency domain.
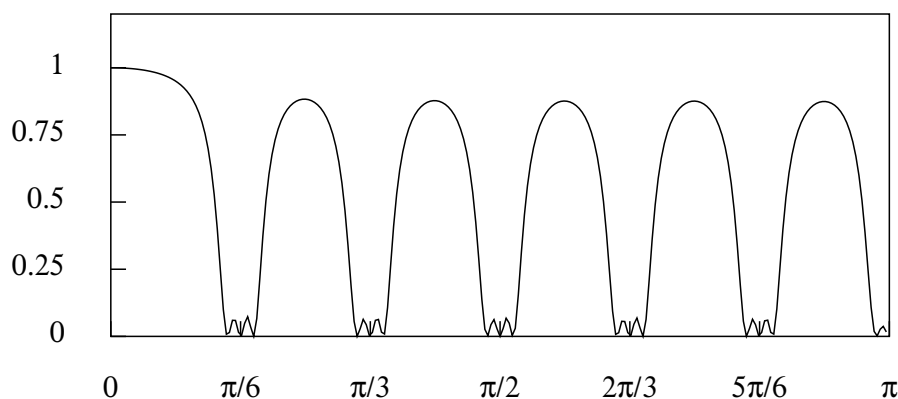

Figure 8 The frequency response function of the triple seasonal adjustment filter for monthly data with offsets of 3 degrees.

Filters for Extracting the Trend-Cycle Function

The economic models that underlie the SEATS-TRAMO and the STAMP programs contain explicit trend functions in the nature of second-order or integrated random walks. These functions give rise to filters that can be used to extract tendcycle functions from the data, which are somewhat smoother than the seasonally adjusted data sequences.

In the seasonal adjustment procedures of the IDEOLOG program, the trend is extracted by a polynomial regression. The regression residuals are then subjected to a seasonal adjustment filter, whereafter they are added back to the polynomial to create the seasonally adjusted data.

The trend extraction filters of the SEATS-TRAMO and the STAMP programs can be mimicked, nevertheless, by applying a low pass smoothing filter to the seasonally adjusted residuals. When the resulting sequence is added to the polynomial trend, the result is similar to those obtained from the above-mentioned programs.

The procedures of the SEATS-TRAMO programs are based on the airline passenger model of Box and Jenkins (1976), which is represented by the equation

$$y(z) = \frac{(1 - \theta z)(1 - \Theta z^s)}{(1 - z)(1 - z^s)} \varepsilon(z) = \frac{(1 - \theta z)(1 - \Theta z^s)}{\nabla^2(z)\Sigma(z)} \varepsilon(z), \tag{23}$$

where $\nabla^2(z) = (1 - z)^2$ is the twofold differencing operator. The parameter values estimated by Box and Jenkins, which are the values that determine the frequency response functions of Figures 9 and 10, are $\theta = 0.4$ and $\Theta = 0.6$.

The program effects a decomposition of the data into a seasonal component, a trend-cycle component and a noise component that are described by statistically independent processes driven by separate white-noise forcing functions. It espouses the principle of canonical decompositions that has been expounded by Hillmer and Tiao (1982).
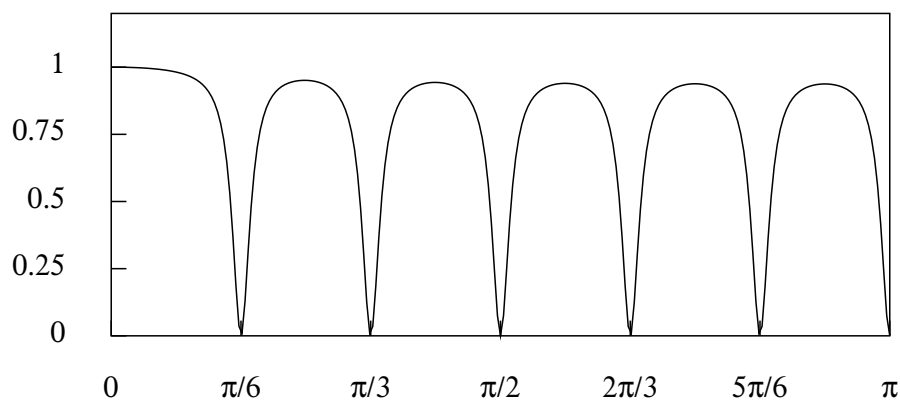

Figure 9. The frequency response of the seasonal-adjustment filter associated with the monthly airline passenger model.
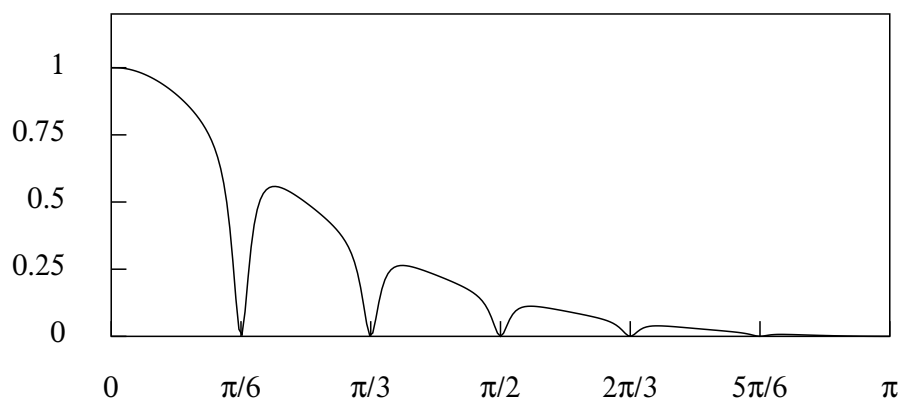

Figure 10. The frequency response of the trend extraction filter associated with the monthly airline passenger model.

12

This principle proposes that any elements of white noise that are present in the seasonal component and the trend component, after an initial decomposition, should be extracted from them and assigned to the noise component. The filters for estimating the trend component and the seasonal component are derived by applying the Wiener–Kolmogorov principle to the revised decomposition.

Thus, the filters can be derived from a *meta-model* defined by the equation

$$y(z) = \frac{U(z)}{\nabla^2(z)}\tau(z) + \frac{V(z)}{\Sigma(z)}\zeta(z) + \eta(z), \tag{24}$$

where $\tau(z)$, $\zeta(z)$ and $\eta(z)$ represent mutually independent white-noise processes and where $U(z)$ and $V(z)$ are polynomials with zeros on the unit circle such as to eliminate the white-noise components within the trend and the seasonal components, which would have uniform spectra over the interval $[0, \pi]$.

Whereas no explicit expressions are available for $U(z)$ and $V(z)$, the expressions for $\Omega_\tau(z) = U(z^{-1})U(z)$ and $\Omega_\zeta(z) = V(z^{-1})V(z)$ have been provided by Hillmer and Tao (1982). On this basis, the trend-extraction filter can be represented by the equation

$$\begin{aligned}
\beta(z) &= \sigma_\tau^2 \frac{U(z^{-1})U(z)}{\nabla^2(z^{-1})\nabla^2(z)} \times \frac{\nabla^2(z^{-1})\Sigma(z^{-1})\Sigma(z)\nabla^2(z)}{\sigma_\varepsilon^2(1 - \theta z^{-1})(1 - \Theta z^{-1})(1 - \Theta z)(1 - \theta z)} \\
&= \frac{\sigma_\tau^2}{\sigma_\varepsilon^2} \frac{\Sigma(z^{-1})\Omega_\tau\Sigma(z)}{(1 - \theta z^{-1})(1 - \Theta z^{-1})(1 - \Theta z)(1 - \theta z)}
\end{aligned} \tag{25}$$

This is a ratio of the autocovariance generating functions of the trend component and of the data. The filter for extracting the seasonal component is constructed likewise. The seasonally adjusted sequence is created by subtracting the estimated seasonal component from the data sequence. Therefore, it may be regarded as a composite of the trend component and the noise component

Figure 9 represents the frequency response function of the seasonal adjustment filter derived from the airline passenger model. It hardly differs from the frequency response function of Figure 3 derived from the heuristic model of (5). Figure 10 represents the frequency response function of the trend extraction filter derived from the airline passenger model.

In order to mimic the trend extraction filter of Figure 10, a smoothing filter based on a second-order moving average $\mu(z) = 1 + \mu_1 z + \mu_2 z^2$ can be applied in series with the seasonal adjustment filter of (13). The smoothing filter is represented by

$$M(z^{-1})M(z) = \frac{(1 + \mu_1 z^{-1} + \mu_2 z^{-2})(1 + \mu_1 z + \mu_2 z^2)}{(1 + \mu_1 + \mu_2)^2}. \tag{26}$$

The purpose of the denominator is to ensure that the filter has a unit at the zero frequency.
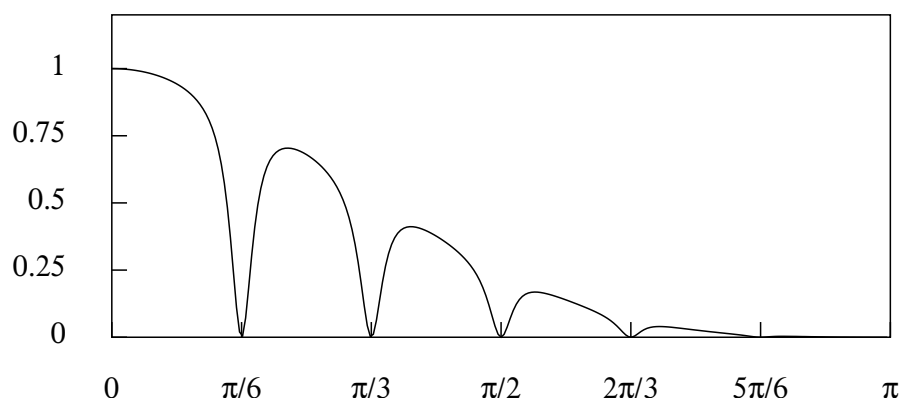
Figure 11. The frequency response of a trend extraction filter that mimicks that of the monthly airline passenger model.

A parsimonious parametrisation of the smoothing filter is achieved by adopting a second-order moving average of the form $1+(1+\kappa)z+\kappa z^2$, with $\kappa \in [0,1]$. Figure 11 shows the frequency response function of a filter that compounds the smoothing filter with the filter of which the frequency response is depicted in Figure 3 by the unbroken line. In this case, The smoothing parameter is $\kappa = 0.6$.

As the frequency value increases, the attenuations are not as severe as those of the frequency response of the airline filter, but a closer correspondence could be achieved at the cost of attributing additional parameters to the smoothing filter. The effect of applying this filter to the quarterly sequence of Figure 4 is shown in Figure 12.
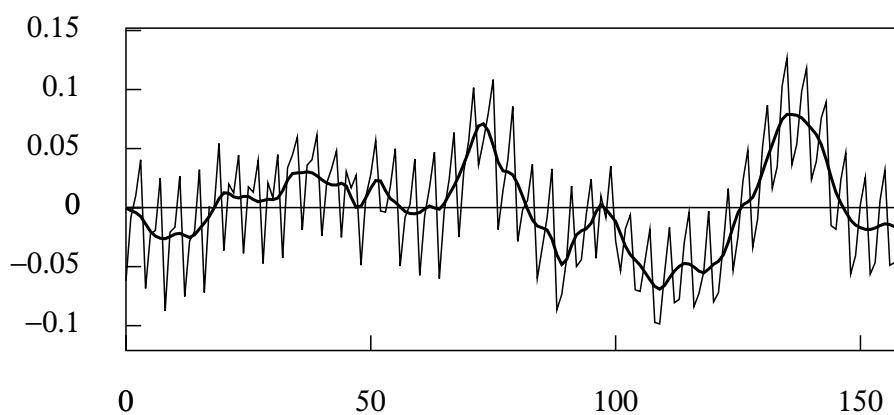

Figure 12. The effect of applying the trend extraction filter to the sequence depicted in Figure 8.

The Frequency-Domain Methods

The methods of seasonal adjustment that operate in the frequency domain are more flexible than the conventional time-domain methods. The Fourier ordinates of a detrended data sequence can be rescaled in any way that is deemed to be

14

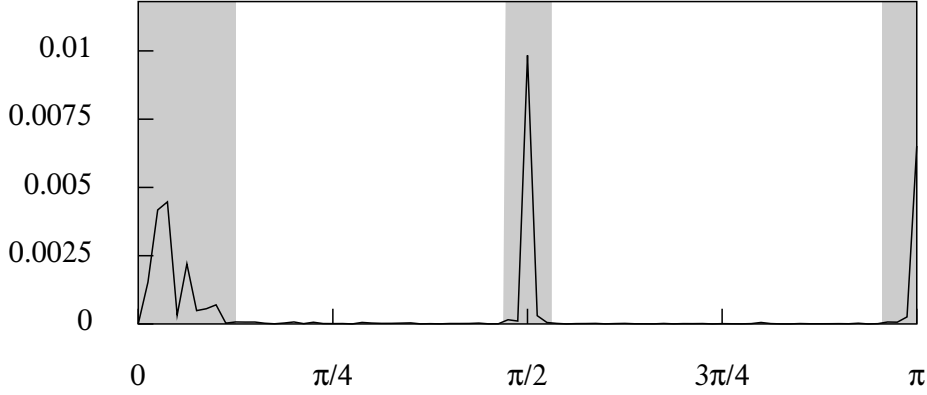appropriate, thereby altering the amplitude of the sinusoidal elements of which the data are composed.

Figure 13. The periodogram of the residual sequence from the linear detrending of the logarithmic consumption data.

A close inspection of the periodogam of the data should indicate which of the elements need to removed or to be attenuated in pursuit of the seasonal adjustment. The effects of the irregularities of the calendar and the effects of strikes and holidays etc. can induce irregularities in the seasonal fluctuations. Then, the fluctuations are liable to comprise elements at frequencies that are adjacent to the seasonal frequency and its harmonics. These can be removed easily by operating in the frequency domain.

In the conventional methods of seasonal adjustment, such irregularities are addressed directly by adjusting the data. Descriptions of the methods have been provided recently by Attal-Toubert *et al.* (2018) and by Ladiray (2018). The methods are complicated, and they require expertise. They can be avoided and the irregularities can be accommodated by operating on the Fourier ordiantes in the frequency domain

The relationships between the data sequence $\{y_t; t = 0, 1, \ldots, T-1\}$ and the Fourier ordinates $\{\zeta_j; j = 0, 1, \ldots, T-1\}$ is represented by

$$y_t = \sum_{j=0}^{T-1} \zeta_j e^{i\omega_j t} \longleftrightarrow \zeta_j = \frac{1}{T} \sum_{t=0}^{T-1} y_t e^{-i\omega_j t}, \qquad \text{with} \qquad \omega_j = \frac{2\pi j}{T}. \tag{27}$$

The first of these equations, which depicts the inverse Fourier transform, represents the Fourier synthesis of the data, whereas the second equation depicts the direct Fourier transform of the data.

The data can also be expressed in terms of a set of mutually orthogonal trigonometric functions:

$$y_t = \sum_{j=0}^{[T/2]} (\alpha_j \cos \omega_j t + \beta_j \sin \omega_j t), \tag{28}$$

where $[T/2]$ is the quotient (i.e. the integral part) of $T/2$. The coefficients of this equation are

$$\alpha_j = \zeta_j + \zeta_{T-j} \qquad \text{and} \qquad i\beta_j = \zeta_{T-j} - \zeta_j, \tag{29}$$

15

whereas, according to Euler's equations, there are

$$\cos\theta = \frac{e^{i\theta} + e^{-i\theta}}{2} \quad \text{and} \quad \sin\theta = \frac{-i}{2}(e^{i\theta} - e^{-i\theta}) = \frac{1}{2i}(e^{i\theta} - e^{-i\theta}). \quad (30)$$

The coefficients of equation (28) are obtained by projecting the data onto the trigonometrical functions. In the case where T is an odd number, this gives

$$\alpha_0 = \frac{1}{T}\sum_t y_t = \bar{y}, \quad \alpha_j = \frac{2}{T}\sum_t y_t \cos\omega_j t \quad \text{and} \quad \beta_j = \frac{2}{T}\sum_t y_t \sin\omega_j t, \quad (31)$$

where $j = 1, \ldots, [T/2] = (T-1)/2$. In the case where T is an even number, the formulae above are valid for $j = 1, \ldots, (T/2) - 1$ and, for $j = n = T/2$, there are

$$\beta_n = 0 \quad \text{and} \quad \alpha_n = \frac{1}{T}\sum_t (-1)^t y_t. \quad (32)$$

In both cases, there is $\beta_0 = 0$.

The Periodogram of the data is the graph of the function function $I(\omega_j) = (T/2)(\alpha_j^2 + \beta_j^2)$. Figure 13 shows the periodogram of the consumption data that are portrayed in Figures 5 and 12.

In this figure, the seasonal elements that it would be appropriate to remove from the data correspond to the highlighted band in the vicinity of $\pi/2$. Apart from the spectral structure that falls within the frequency interval $[0, \pi/8]$, there is little else in the data. Nevertheless, there is noise in the data that falls within the deadspaces that occupy the remainder of the frequency axis. Therefore, it is appropriate to represent the business cycle by a synthesis of the sinusoidal elements that lie in the interval $[0, \pi/8]$. The result is represented in Figure 14.
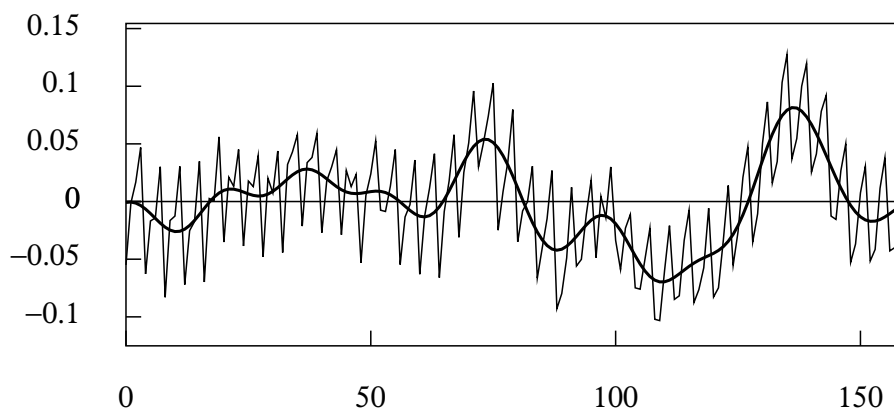

Figure 14. The residual sequence from fitting a linear trend to the logarithmic consumption data with an interpolated line representing the business cycle, obtained by the frequency-domain method.

This representation of the business cycle is liable to be preferred to that of Figure 12 which has been produced by a time-domain method and which is affected

16

by some of the noise from within the deadspaces and by some proportion of the elements that are adjacent to the seasonal frequencies.

The difference between the smooth trajectory of Figure 14 and the rough seasonally adjusted sequence of Figure 5 appears to be only noise that is devoid of any economic information. Therefore, it can be argued that the estimated trend-cycle sequence of Figure 14 should serve for the seasonally adjusted data.

Stop Bands and Transition Bands

The advantage of the frequency-domain method of seasonal adjustment is that it allows complete flexibility in determining an appropriate frequency response for eliminating the seasonal effects from the data. The simplest design is one in which the stop bands, which eliminate the seasonal elements of the data, have zero gain and in which the pass bands, which preserve all other elements, have unit gain.

The extent of the stop bands, which cover the seasonal frequency and its harmonic frequencies, can be determined in the light of the periodogram of the detended data. The elements adjacent to those of the seasonal frequencies, which might be thought to contribute to the seasonal fluctuations, can also be covered by the stop bands, albeit that, alternatively, they can be partially attenuated within adjacent transition bands. In Figure 13, the clefts that surround the seasonal frequencies are vertical shafts, and there are no transition bands.

It is possible to define transition bands that allow a gradual transition between the pass bands and the stop bands. The trajectory of the frequency response within these bands must make a monotonic transition from unity to zero and vice versa; but, otherwise, its precise nature is a matter of choice. The *SEASCAPE* program offers four choices. The first choice is not to have any transition bands and to allow the frequency response to pass abruptly between unity and zero and vice versa.
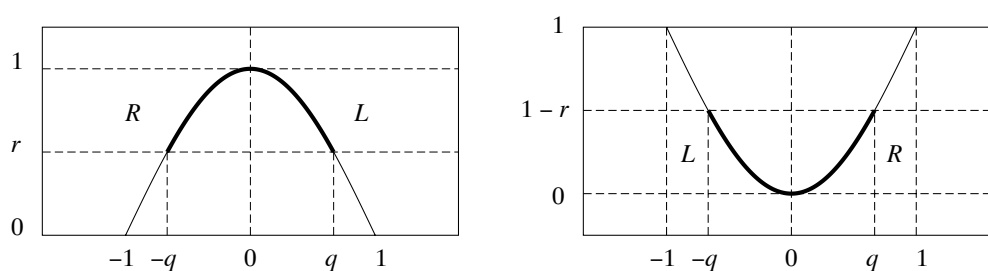

Figure 15. The cosine segments that give rise to the *lower-half cosine transitions,* (left) and the *lower-half cosine transitions,* (right).

The second possibility is to govern the transitions by segments of a cosine function restricted to the intervals $L = [0, q \leq \pi/2]$ and $R = [-q \geq -\pi/2, 0]$. The transition on L (L for left) from the pass band to the stop band occurs when $x \in [0, q]$ and the transition R (R for right) from the stop band to the pass band occurs when $x \in [-q, 0]$. Thus, the *upper-half cosine transitions* are generated by

the function

$$\frac{1}{1-r}\{\cos(x^n\pi/2) - r\} \quad \text{with} \quad x \in [0, q] \quad \text{and} \quad x \in [-q, 0], \tag{33}$$

$$\text{where} \quad r = \cos(q^n\pi/2).$$

Here, $q \in [0.5, 1]$ is a parameter that adjusts the shape of the transitions by abbreviating them. The integer $n \in [1, 6]$ affects the curvature at the beginning of the transitions, which become more gradual as n increases, whereas the descent, or the ascent, which is delayed, becomes more rapid. The formulation of (33) is readily intelligible when $q = 1$ and $r = 0$. When $r \neq 0$, the formulation can be understood in the light of the left side Figure 15.

The third choice, which is described as the *lower-half cosine transitions,* employs the function

$$\frac{1}{1-r}\{1 - \cos(x^n\pi/2)\} \quad \text{with} \quad x \in [-q, 0] \quad \text{and} \quad x \in [0, q], \tag{34}$$

$$\text{where} \quad r = \cos(q^n\pi/2).$$

Here, the transition L from pass band to stop band occur when $x \in [-q, 0]$ and the transition R from the stop band to the pass band occurs when $x \in [0, q]$. The right side of Figure 15 elucidates this formulation.

To complete these specifications, there must be mappings from the frequency index $\omega \in [0, \pi]$ to the variable x that governs frequency response within the clefts that comprise the transition bands the stop bands. A sub-interval of $[0, \pi]$ on which a cleft is defined takes form of

$$[M_a, M_b, M_c, M_d], \tag{35}$$

where $[M_a, M_b]$ and $[M_c, M_d]$ are left and right transition bands respectively and $[M_b, M_c]$ is the stop band. Then, in the case of the *upper-half cosine transitions* of (33), there will be

$$L: \quad x = \frac{q\{\omega - M_a\}}{M_b - M_a} \quad \text{if} \quad \omega \in [M_a, M_b] \quad \text{and}$$
$$R: \quad x = \frac{q\{\omega - M_c\}}{M_c - M_d} \quad \text{if} \quad \omega \in [M_c, M_d]. \tag{36}$$

whereas, in the case of the *lower-half cosine transition* of (34), there are

$$L: \quad x = \frac{q\{\omega - M_b\}}{M_b - M_a} \quad \text{if} \quad \omega \in [M_a, M_b] \quad \text{and}$$
$$R: \quad x = \frac{q\{\omega - M_c\}}{M_d - M_c} \quad \text{if} \quad \omega \in [M_c, M_d]. \tag{37}$$

A fouth choice is to govern the transitions by a sigmoid or logistic function. There are numerous functions that might be employed, were it not for the fact

that they reach their asymptotes as $x \to \pm\infty$. For present purposes, the sigmoid functions must reach their upper and lower levels at the boundaries of the transition regions. A flexible function that satisfies this requirement can be formed by joining the upper an lower cosine transition functions.

The *left-side composite sigmoid function* is defined as a function of $z = 0 \to 2$ comprising two segments as follows:

$$
\begin{aligned}
L_a(z): &\quad \{\cos(x^n \pi/2) + 1\}/2 \quad \text{with} \quad x = z \quad \text{when} \quad z \in [0, 1], \\
L_b(z): &\quad \{1 - \cos(x^n \pi/2)1\}/2 \quad \text{with} \quad x = 2 - z \quad \text{when} \quad z \in [1, 2].
\end{aligned}
\tag{38}
$$

The segments join seamlessly when $z = 1$. The *right-side function,* is obtained when $z = 2 \to 0$ is run in reverse.

If there is a requirement to mimic the effects of one of the time-domain filters, then it will be appropriate to employ the upper-half cosine transitions. An example is provided by the triple time-domain filter of which the frequency response is portrayed in Figure 8. The frequency response of a frequency-domain version of the filter is shown in Figure 16.
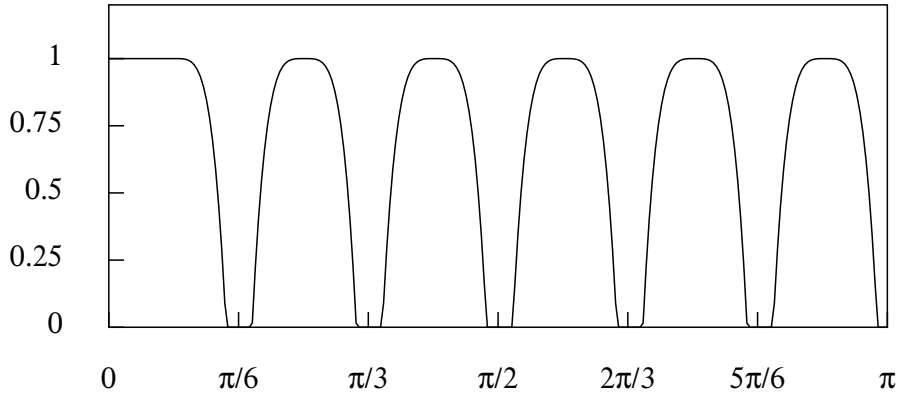

Figure 16. The frequency response function of a frequency-domain seasonal adjustment filter for monthly data with stop bands of 6 degrees in width.

There are some manifest differences in the two frequency responses. The frequency-domain filter shows no leakage in the stop bands. The gain of the filter in the regions between the stop bands reaches unity, with the effect that the non-seasonal components are suffering from less attenuation than in the case of the time-domain filter. These features can be counted as advantages. However, it is unclear why this filter should be preferred to one that makes abrupt transitions between the pass bands and the stop bands.
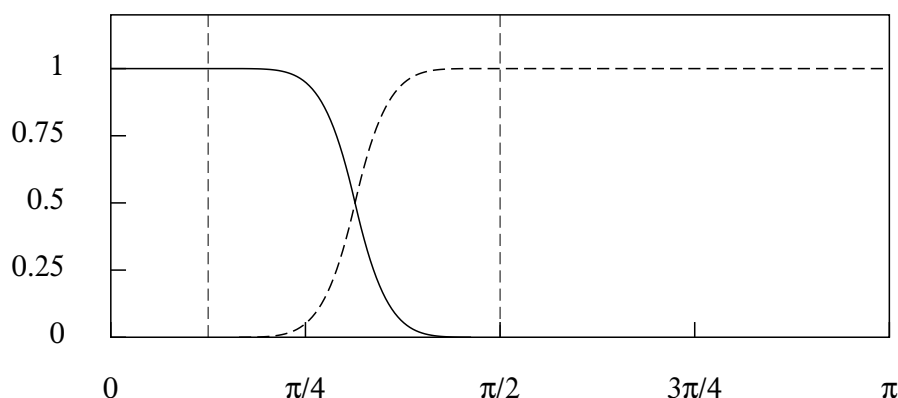
Figure 17. The frequency response function of a low pass frequency-domain filter with a transition in the interval $[\pi/8, \pi/2]$ governed by a composite sigmoid function with $n = 3$.

The *left-side composite function* will serve for the transition band of a low pass filter. The *right-side function* will serve for the transition band of a high pass filter. Figure 17 shows, via the continuous line, the frequency response of a lowpass filter. It shows, via the dashed line, the frequency response of the complementary highpass filter. The sum of the two frequency responses is unity, which implies that the complementary filters partition the data.

The low pass filter, of which the frequency response resembles that of the Butterworth filter, will serve to isolate a trend-cycle function. The rate of transition can be increased either by raising the value of n or by narrowing the transition band, or by both. For an account of the finite-sample Butterworth filter, see Pollock (2000).

References

Attal-Toubert, K., D. Ladiray, M., Marini and J. Palate, (2018), Moving Trading-Day Effects with X-13 ARIMA-SEATS and TRAMO-SEATS, Chapter 6 in Mazzi, G.L., D. Ladiray, and D.A. Rieser, (eds.), *Handbook on Seasonal Adjustment 2018 edition,* Eurostat: Publications Office of the European Union, Luxembourg.

Box, G.E.P., and G.M. Jenkins, (1976), *Time Series Analysis: Forecasting and Control, Revised Edition,* Holden Day, San Francisco.

Caporello G., and A. Maravall, (2004), *Program TSW, Revised Reference Manual,* Servicio de Estudios, Banco de España.

Findley, D.F., T.S. McElroy and K.C. Wills, (2005), Modifications of SEATS' Diagnostic for Detecting Over- or Underestimation of Seasonal Adjustment Decomposition Components, U.S. Census Bureau.

Gómez, V., and A. Maravall, (1997), *TRAMO (Time Series Regression with ARIMA Noise, Missing Observations, and Outliers) and SEATS (Signal Extraction in ARIMA Time Series) Instructions for the User,* Banco de España, Madrid.

Gómez, V., and A. Maravall, (2001), Seasonal Adjustment and Signal Extraction in Economic Time Series, chapter 8 in D. Peña, G.C. Tiao, and R.S. Tsay (eds.), *A Course in Time Series Analysis,* John Wiley and Sons, New York.

Hillmer, S.C., and G.C. Tiao, (1982), An ARIMA-Model-Based Approach to Seasonal Adjustment, *Journal of the American Statistical Association,* 77, 63–70.

Kaiser, R., and A. Maravall, (2001), *Measuring Business Cycles in Economic Time Series,* Lecture Notes in Statistics 154, Springer-Verlag, New York.

Ladiray, D., (2018), Calendar Effects, Chapter 5 in in Mazzi, G.L., D. Ladiray, and D.A. Rieser, (eds.), *Handbook on Seasonal Adjustment 2018 edition,* Eurostat: Publications Office of the European Union, Luxembourg.

Ladiray, D., and B. Quenneville, (2001), *Seasonal Adjustment with the X-11 Method,* Springer Lecture Notes in Statistics 158, Springer Verlag, Berlin.

Mazzi, G.L., D. Ladiray, and D.A. Rieser, (2018), Handbook on Seasonal Adjustment 2018 Edition, Eurostat: Publications Office of the European Union, Luxembourg.

McElroy, T., and A. Roy, (2017), Detection of Seasonality in the Frequency Domain, Center for Statistical Research & Methodology Research and Methodology Directorate U.S. Census Bureau, Washington.

Pollock, D.S.G., (2000), Trend Estimation and De-Trending via Rational Square Wave Filters, *Journal of Econometrics,* 99, 317–334.

Shiskin, J., A.H. Young, and J.C. Musgrave, (1967), *The X-11 Variant of the Census Method II Seasonal Adjustment,* Technical Paper No. 15, Bureau of the Census, U.S. Department of Commerce.